

Synthesis and Structure of a Seven-Coordinate Molybdenum Carbonyl Fluoride Derivative: $[\text{Et}_4\text{N}][\text{Mo}(\text{CO})_2(\text{S}_2\text{CNEt}_2)_2\text{F}]$

S. J. N. BURGMAYER and J. L. TEMPLETON*

Received July 5, 1984

An improved preparative route into molybdenum(II) and tungsten(II) dithiocarbamate chemistry has been developed that proceeds through $[\text{M}(\text{CO})_5\text{I}]^-$ and $[\text{M}(\text{CO})_4\text{I}_3]^-$. Addition of fluoride or azide ion to $\text{M}(\text{CO})_2(\text{S}_2\text{CNR}_2)_2$ ($\text{M} = \text{Mo}, \text{W}$) yields $[\text{M}(\text{CO})_2\text{X}(\text{S}_2\text{CNR}_2)_2]^-$ ($\text{X} = \text{F}, \text{N}_3$). The structure of $[\text{Et}_4\text{N}][\text{Mo}(\text{CO})_2(\text{S}_2\text{CNEt}_2)_2\text{F}]$ (**1**), a rare molybdenum(II) carbonyl fluoride complex, is reported with crystallographic parameters of $a = 11.152$ (4) Å, $b = 16.039$ (5) Å, $c = 15.846$ (4) Å, $\beta = 91.91$ (2)°, and $Z = 4$ defining a monoclinic lattice of space group $P2_1/n$. Refinement to $R_1 = 4.7\%$ and $R_2 = 3.4\%$ was attained. The idealized geometry of **1** is that of a capped trigonal prism where fluoride occupies the capping site trans to both carbonyl groups. The structure of **1** exhibits an acute OC-M-CO angle of 67.4°, and extended Hückel calculations on $\text{Mo}(\text{CO})_2(\text{S}_2\text{CNR}_2)_2$ (OC-M-CO = 74.3°) and the fluoride complex **1** have been performed to probe factors that influence this angle.

Introduction

Well characterized 16-electron complexes serve as models for reactive intermediates. At least one strongly π -basic ligand is found in virtually all isolated 16-electron early-transition-metal carbonyl monomers. The general relationship of π -base interactions to the stability of unsaturated six-coordinate molecules is clear.¹ Alkyne ligands are conspicuous for their ability to stabilize formal 16-electron monomers. The reluctance of these complexes to add a seventh ligand reflects the large HOMO-LUMO gap promoted by the alkyne π basicity.²

The 16-electron $\text{Mo}(\text{CO})_2(\text{S}_2\text{CNR}_2)_2$ monomers were first reported 16 years ago;³ a structural study revealed an unusual trigonal-prismatic geometry.⁴ Since $\text{Mo}(\text{CO})_2(\text{S}_2\text{CNR}_2)_2$ exhibits only a moderate tendency to coordinate a seventh ligand, it is suitable for equilibrium studies of ligand additions. We have previously quantified this electrophilicity and structurally examined one seven-coordinate product, $\text{Mo}(\text{CO})_2(\text{S}_2\text{CNEt}_2)_2(\text{tht})$ ($\text{tht} = \text{SC}_4\text{H}_8$).⁵ The site occupied by tht was consistent with the idea that ligand addition to $\text{Mo}(\text{CO})_2(\text{S}_2\text{CNR}_2)_2$ is frontier orbital controlled. The principles of orbital-directed reactions set forth by Fukui⁶ are applicable in organometallic chemistry.⁷

The contrast between the geometry of $\text{Mo}(\text{CO})_2(\text{S}_2\text{CNEt}_2)_2$ (tht) and other known $\text{M}(\text{CO})_2(\text{S}_2\text{CNR}_2)_2\text{L}$ structures ($\text{M} = \text{W}$; $\text{L} = \text{CO}, \text{PPh}_3$)⁸ raised several questions. Is the geometry of the adduct with $\text{L} = \text{tht}$ solely due to the weak bonding of tht to the metal? Would a stronger M-L bond to the seventh ligand promote rearrangement to the mutually *cis*- $\text{M}(\text{CO})_2\text{L}$ unit observed for $\text{L} = \text{CO}$ and PPh_3 ? Are differences in the π -acid properties of the added ligand responsible for the ultimate seven-coordinate geometry? These queries led us to the preparation and structure determination reported herein for the seven-coordinate $[\text{Et}_4\text{N}][\text{Mo}(\text{CO})_2(\text{S}_2\text{CNEt}_2)_2\text{F}]$ complex. Since we have interests in carbonyl fluorides in general and in building $d^4 L_5\text{M}(\text{CO})_2$ complexes with particularly acute OC-M-CO angles,¹⁰ the $[\text{Mo}(\text{CO})_2(\text{S}_2\text{CNEt}_2)_2\text{F}]^-$ anion was an obvious choice for a structural study. Extended Hückel (EHMO) calculations have

been used to probe the origin of the OC-M-CO angle of 67.4° in this fluoride adduct, since an acute OC-M-CO angle may be important in efforts to promote carbon-carbon bond formation through reductive carbonyl coupling. An improved synthetic pathway into Mo(II) and W(II) dithiocarbamate chemistry is also reported. This work adds to the extensive seven-coordinate chemistry of $\text{ML}_3(\text{S}_2\text{CNR}_2)_2$ compounds now extant.^{11,13}

Experimental Section

Materials and Methods. Unless otherwise noted, all manipulations were done under purified nitrogen on a vacuum line with use of standard Schlenk techniques. Metal carbonyls, tetraalkylammonium halide salts, and sodium dialkyldithiocarbamate trihydrates were used as received. Bis(triphenylphosphine)nitrogen(1+) (PPN) azide was prepared by anion exchange of sodium azide and $[\text{PPN}][\text{Cl}]$. Infrared spectra were recorded on a Beckman 4250 spectrophotometer. ¹H NMR spectral measurements were made on a Varian XL 100-MHz instrument.

Syntheses. $\text{Mo}(\text{CO})_2(\text{S}_2\text{CNR}_2)_2$ ($\text{R} = \text{Me}, \text{Et}$). (a) **Formation of $[\text{Et}_4\text{N}][\text{Mo}(\text{CO})_5\text{I}]$.** $\text{Mo}(\text{CO})_6$ (9.08 g, 0.0344 mol) and 9.19 g (0.0359 mol) of tetraethylammonium iodide, $[\text{Et}_4\text{N}][\text{I}]$, were charged into a 500-mL round-bottom flask. The solids were purged of oxygen through a minimum of three evacuation/nitrogen refill cycles, and then 100 mL of deaerated THF was added. The resultant slurry was refluxed 75 min until all the $\text{Mo}(\text{CO})_6$ was dissolved; the solution was a bright yellow, and no further carbon monoxide was evolved. The solution was cooled; precipitation of yellow crystals of $[\text{Et}_4\text{N}][\text{Mo}(\text{CO})_5\text{I}]$ was induced by addition of 150 mL of diethyl ether followed by chilling to 0 °C. The product was isolated by filtration and washed with Et_2O (2×50 mL). A second crop of product was obtained by concentration of the THF filtrate and addition of Et_2O to yield 19.00 g (95%). IR (THF): ν_{CO} 2052 w, 1929 s, 1863 s cm^{-1} . This product is air-stable for short periods of time and may be isolated in the atmosphere with use of Buchner filtration techniques. $[\text{Et}_4\text{N}][\text{Mo}(\text{CO})_5\text{I}]$ is best stored under a nitrogen atmosphere and will keep indefinitely. The above procedure is also applicable for preparation of other tetraalkylammonium halide derivatives, but we have found that tetraethyl- and tetrapropylammonium cations work best in the following steps.

(b) **Oxidation of $[\text{Mo}(\text{CO})_5\text{I}]^-$ to $[\text{Mo}(\text{CO})_4\text{I}_3]^-$: S_2CNR_2^- Substitution of I^- .** $[\text{Et}_4\text{N}][\text{Mo}(\text{CO})_5\text{I}]$ (9.88 g, 0.020 mol) was dissolved in 120 mL of deaerated methanol. Elemental iodine (5.08 g, 0.020 mol) was added slowly over 5 min to the yellow solution. Vigorous CO evolution accompanied a color change to yellow-orange, indicating $[\text{Mo}(\text{CO})_4\text{I}_3]^-$ formation. Stirring was continued for 20 min until no more gas evolved and all the solid iodine had been consumed. Sodium dialkyldithiocarbamate was added (2 equiv) under a moderate nitrogen flow, causing vigorous production of gaseous CO and an immediate color change to bright orange. Orange crystalline $\text{Mo}(\text{CO})_3(\text{S}_2\text{CNR}_2)_2$ precipitated from the methanolic solution, but as nitrogen was bubbled through the solution

- Templeton, J. L.; Winston, P. B.; Ward, B. C. *J. Am. Chem. Soc.* **1981**, *103*, 7713.
- Herrick, R. S.; Leazer, D. M.; Templeton, J. L. *Organometallics* **1983**, *2*, 834.
- Colton, R.; Scollary, G. R.; Tomkins, I. B. *Aust. J. Chem.* **1968**, *21*, 15.
- Templeton, J. L.; Ward, B. C. *J. Am. Chem. Soc.* **1980**, *102*, 6568.
- Templeton, J. L.; Burgmayer, S. J. N. *Organometallics* **1982**, *1*, 1007.
- Fukui, K. "Theory of Orientation and Stereoselection"; Springer-Verlag: Berlin, 1975.
- (a) Block, T. F.; Fenske, R. F.; Casey, C. P. *J. Am. Chem. Soc.* **1976**, *98*, 441. (b) Kostic, N. M.; Fenske, R. F. *Ibid.* **1981**, *103*, 4677. (c) Eisenstein, O.; Hoffmann, R. *Ibid.* **1981**, *103*, 4308.
- Ward, B. C.; Templeton, J. L. *Inorg. Chem.* **1980**, *19*, 1753.
- Ward, B. C.; Templeton, J. L. *J. Am. Chem. Soc.* **1981**, *103*, 3743.
- Hoffmann, R.; Wilker, C. N.; Lippard, S. J.; Templeton, J. L.; Brower, D. C. *J. Am. Chem. Soc.* **1983**, *105*, 146.

- (a) Chen, G. J.-J.; Yelton, R. O.; McDonald, J. W. *Inorg. Chim. Acta* **1977**, *22*, 249. (b) Carmona, E.; Doppert, K.; Marin, J. M.; Poveda, M. L.; Sanchez, L.; Sanchez-Delgado, R. *Inorg. Chem.* **1984**, *23*, 530. (c) Dilworth, J. R.; Neaves, B. D.; Pickett, C. J.; Chatt, J.; Zubieta, J. A. *Inorg. Chem.* **1983**, *22*, 3524. (d) Colton, R.; Rose, G. G. *Aust. J. Chem.* **1970**, *23*, 1111.
- Templeton, J. L. *Adv. Chem. Ser.* **1979**, *173*, 263.
- Broomhead, J. A.; Young, C. G. *Aust. J. Chem.* **1982**, *35*, 277.

Mo(CO)₂(S₂CNR₂)₂ formed. Since Mo(CO)₂(S₂CNR₂)₂ is completely insoluble in methanol, it was isolated by filtering off the methanolic supernatant and purified by washing with methanol (3 × 50 mL) to remove residual salts (NaI and Et₄NI). This procedure yields 70–75% Mo(CO)₂(S₂CNR₂)₂,^{3,4} a highly air-sensitive purple solid that must be stored under nitrogen.

W(CO)₃(S₂CNR₂)₂ (R = Me, Et). (a) [Et₄N][W(CO)₃I] (or the [n-Pr₄N] salt) may be prepared by following the procedure given above for [Et₄N][Mo(CO)₃I] by substituting chlorobenzene for THF as solvent and allowing a reflux period of 2 h. The reaction is complete when the intensely yellow solution no longer evolves CO.

(b) [Et₄N][W(CO)₃I₃] was prepared as was [Et₄N][Mo(CO)₃I₃]. Subsequent addition of sodium dialkyldithiocarbamates (2 equiv) in methanol formed orange W(CO)₃(S₂CNR₂)₂, which partially precipitated from solution. One hour of stirring allowed complete substitution of dithiocarbamate for iodide. Due to the solubility of W(CO)₃(S₂CNR₂)₂ in methanol, it is not recommended that this orange precipitate be isolated by simple decantation of the methanolic solution of NaI and Et₄NI salts as is possible for Mo(CO)₃(S₂CNR₂)₂. Pure W(CO)₃(S₂CNR₂)₂ was best obtained by evaporation of all solvent in vacuo to dryness. Extraction of W(CO)₃(S₂CNR₂)₂ into toluene followed by filtration to remove salts, concentration of toluene extracts, and addition of 2 volumes of hexanes produced orange-red crystals of W(CO)₃(S₂CNR₂)₂ in ca. 70% yield. W(CO)₃(S₂CNR₂)₂ has previously been spectroscopically¹² and structurally⁸ characterized.

W(CO)₂(S₂CNR₂)₂ (R = Me, Et, *i*-Pr). Loss of one CO from W(CO)₃(S₂CNR₂)₂ occurs when the tricarbonyl complexes are refluxed in methanol for 1 h, as reported by Broomhead and Young.¹³

[Et₄N][Mo(CO)₂(S₂CNEt₂)₂F] (1). Mo(CO)₂(S₂CNEt₂)₂ (0.45 g, 1.0 mmol) was charged into a 100-mL round-bottom flask in the drybox. An excess of [Et₄N][F]·2H₂O (1.5 mmol) was added while maintaining a moderate nitrogen flow. The solids were purged of oxygen with several evacuation/N₂ cycles. Methylene chloride (20 mL) was dripped into the flask. The resulting solution was stirred 15 min, during which time the purple color of Mo(CO)₂(S₂CNEt₂)₂ gradually changed to the brilliant orange of 1 as the ammonium fluoride hydrate dissolved. The reaction was monitored by solution IR spectra. The CH₂Cl₂ solution was chilled to 0 °C to precipitate excess fluoride salt and to freeze out the water of hydration; these were removed by filtration. Precipitation of orange needles was induced by layering deoxygenated Et₂O over the CH₂Cl₂ solution and allowing slow diffusion of the two phases. Isolation of 1 yielded 0.52 g (88%). IR (KBr): ν_{CO} 1884, 1797; ν_{CN} 1487; ν_{MoF} 413 cm⁻¹. IR (CH₂Cl₂): ν_{CO} 1895; 1807 cm⁻¹. ¹H NMR (CD₂Cl₂): δ 3.64 (dq, 8 H, -CH₂(S₂CNEt₂), J_{HF} = 2 Hz), 3.33 (q, 8 H, -CH₂(Et₄N)), 1.20 (t, 24 H, -CH₃(Et₄N and S₂CNEt₂)).

[Et₄N][W(CO)₂(S₂CNR₂)₂F] (2a, R = Me; 2b, R = Et). The same procedure as for 1 above produces an 83% yield of orange 2a and 2b. When W(CO)₂(S₂CNMe₂)₂ is used, however, the observed color change is from green to orange. 2a: IR (CH₂Cl₂) ν_{CO} 1879, 1775 cm⁻¹. 2b: IR (CH₂Cl₂) ν_{CO} 1874, 1781 cm⁻¹; IR (KBr) ν_{CO} 1864, 1773, ν_{CN} 1488, ν_{WF} 420 cm⁻¹; ¹H NMR (CD₂Cl₂) δ 3.59 (dq, 8 H, -CH₂(S₂CNEt₂), J_{HF} = 3 Hz), 3.30 (q, 8 H, -CH₂(Et₄N)), 1.30 (t, 24 H, -CH₃(Et₄N and S₂CNEt₂)).

[PPN][M(CO)₂(S₂CNEt₂)₂N₃] (M = Mo (3), W (4)). A procedure similar to the preparation of 1 was followed for syntheses of azide complexes 3 and 4 except that a stoichiometric addition of PPN azide salt was used. Upon addition of methylene chloride to the dry purged solids, an immediate reaction produced 3 and 4; crystallization was induced with Et₂O. Filtration and washing with ether (2 × 25 mL) produce quantitative yields of 3 and 4. The stability of these complexes to oxygen and moisture is significantly greater than that of the fluoride analogues; 4 may be handled as a solid in air for brief periods (30 min) without noticeable decomposition. 3: IR (CH₂Cl₂) ν_{CO} 1908, 1820, ν_{NN} 2040 cm⁻¹; IR (KBr) ν_{CO} 1898, 1814, ν_{NNN} 2030, ν_{CN} 1485 cm⁻¹; ¹H NMR (CD₂Cl₂) δ 7.52 (br, 30 H, -Ph), 3.68 (q, 8 H, -CH₂(S₂CNEt₂)), 1.20 (t, 12 H, -CH₃). 4: IR (CH₂Cl₂) ν_{CO} 1892, 1798, ν_{NNN} 2050 cm⁻¹; IR (KBr) ν_{CO} 1885, 1796, ν_{NNN} 2045, ν_{CN} 1487 cm⁻¹; ¹H NMR (CD₂Cl₂) δ 7.52 (br, 30 H, -Ph), 3.56 (q, 8 H, -CH₂(S₂CNEt₂)), 1.20 (t, 12 H, -CH₃).

Structure Determination of [Et₄N][Mo(CO)₂(S₂CNEt₂)₂F] (1). (a) **Data Collection.** Bright orange crystals of 1 were grown by slow diffusion of THF layered over a methylene chloride solution of 1. The crystal selected for study was loaded into a capillary tube under a nitrogen atmosphere; the capillary was sealed with epoxy while still under nitrogen. Approximate crystal dimensions were 0.35 × 0.40 × 0.50 mm. Diffraction data were collected on an Enraf-Nonius CAD-4 automatic diffractometer (see Table I).¹⁴ Centering and least-squares refinement

Table I. Crystallographic Data and Collection Parameters for [Et₄N][Mo(CO)₂(S₂CNEt₂)₂F]

space group	P2 ₁ /n
a, Å	11.152 (4)
b, Å	16.039 (5)
c, Å	15.846 (4)
β, deg	91.91 (2)
V, Å ³	2833 (3)
d(calcd), g/cm ³	1.402
Z	4
fw	597.8
μ, cm ⁻¹ (abs coeff)	7.665
radiation	Mo Kα (λ = 0.710 73 Å)
temp, °C	22
monochromator	graphite cryst
scan range, deg	2 < 2θ < 52
data collected	+h,+k,±l
scan width, deg	1.0 + (0.35 tan θ)
bkgd scan width	25% of full pk width on each side
no. of unique data	5546
no. of data, I > 3σ(I)	2304
no. of variables	289
R ₁	0.047
R ₂	0.034
error in observn of unit wt	1.58

Table II. Extended Hückel Calculation Parameters

atom	orbital	H _{ii} , eV	e ₁ (C ₁) ^a	e ₂ (C ₂)
H	1s	-13.60	1.300	
C	2s	-21.40	1.625	
	2p	-11.40	1.625	
N	2s	-26.00	1.950	
	2p	-13.40	1.950	
O	2s	-32.30	2.275	
	2p	-14.80	2.275	
F	2s	-40.00	2.600	
	2p	-18.10	2.600	
S	3s	-20.00	1.817	
	3p	-13.30	1.817	
Mo	5s	-8.77	1.930	
	5p	-5.60	1.930	
	4d	-10.06	4.540 (0.5899)	1.90 (0.5899)

^a Values taken from ref 15b,c.

of 25 reflections found in the region 15° < θ < 17° indicated a monoclinic lattice with a = 11.152 (4) Å, b = 16.039 (5) Å, c = 15.846 (4) Å and β = 91.91 (2)° defining a cell volume of 2833 (3) Å³. C₂₀H₄₀FMoN₃O₂S₄ has a molecular weight of 597.8. The calculated density is 1.402 g/cm³ for Z = 4. Diffraction data with Mo Kα radiation (λ = 0.710 73 Å) were collected in the quadrant +h,+k,±l for 1° < θ < 26°. Three strong reflections monitored every 4 h showed no significant decay; orientation was checked after every 300 reflections. A total of 5546 unique data were collected. Systematic absences observed for h + l ≠ 2n, h0l, and k ≠ 2n, 0k0, suggested the space group P2₁/n, which was confirmed by subsequent refinement of the structural model.

(b) **Solution and Refinement.** The molybdenum position was obtained from inspection of the Patterson map. Least-squares refinement and difference Fourier calculations produced locations of all other non-hydrogen atoms. One methyl carbon (C12) of a diethyldithiocarbamate ligand showed a twofold rotational disorder and was best refined when each site was assigned 50% occupancy (based on the equivalent peak heights observed for each location in the difference Fourier map).

(14) (a) Programs were utilized during solution and refinement as provided in the Enraf-Nonius structure determination package; scattering factors are taken from: Cromer, D. T.; Waber, J. T. "International Tables for X-ray Crystallography"; Ibers, J. A., Hamilton, W., Eds.; Kynoch Press: Birmingham, England, 1974; Vol. IV. (b) I = S(C + RB) and σ(I) = (2S²(C + RB) + (ρI)²)^{1/2}, where S = scan rate, C = total integrated peak count, R = ratio of scan count time to background count time, B = total background count time, and ρ = 0.01 is a correction factor. (c) The function minimized was Σw(|F_o - |F_c||²), where w = [2F_o/σ(F_o)²]² and σ(F_o)² = [σ²(I) + ρ²I²]^{1/2} with ρ assigned a value of 0.01. Expressions for residuals are R₁ = Σ||F_o - |F_c||/Σ|F_o| and R₂ = [Σw(|F_o - |F_c||²)/Σw(F_o)²]^{1/2}.

Though the crystal showed low absorption ($\mu = 7.66 \text{ cm}^{-1}$), an empirical absorption correction was applied to the data prior to the final stages of refinement with transmission factors ranging from 0.95 to 1.00. Hydrogen positions were calculated with $C-H = 0.95 \text{ \AA}$ and included in refinement but not varied. Full-matrix least-squares refinement of the model using anisotropic parameters for all 32 non-hydrogen atoms converged when the largest parameter shift was 1.67, with use of 2304 data where $I > 3\sigma(I)^{14b}$ for 289 variables. The residuals produced^{14c} $R_1 = 0.047$ and $R_2 = 0.034$; the highest peak observed in a difference Fourier calculation at this point was 0.25 e/\AA^3 .

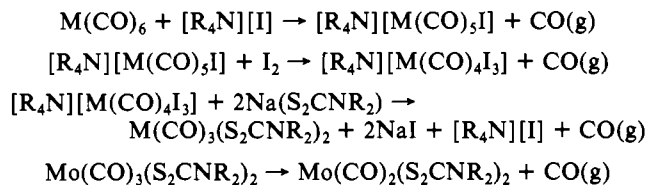
Theoretical Calculations. Extended Hückel calculations as described by Hoffmann¹⁵ were performed on $\text{Mo}(\text{CO})_2(\text{S}_2\text{CNR}_2)_2$ and $[\text{Mo}(\text{CO})_2(\text{S}_2\text{CNR}_2)_2\text{F}]^-$ with use of the parameters in Table II. Program QCPE 358 from the Quantum Chemistry Program Exchange was employed for this calculation. The geometry was defined by the crystallographic coordinates of **1** and $\text{Mo}(\text{CO})_2(\text{S}_2\text{CNR}_2)_2$, where the ethyl groups of diethyldithiocarbamate ligands were replaced with hydrogens set 1.02 \AA from the nitrogen atoms.

Results

Syntheses. Preparation of $\text{Mo}(\text{CO})_2(\text{S}_2\text{CNR}_2)_2$ and $\text{W}(\text{CO})_3(\text{S}_2\text{CNR}_2)_2$ (Scheme I) proceeds through thermal CO substitution of molybdenum or tungsten hexacarbonyl by tetraalkylammonium iodide, yielding $[\text{R}_4\text{N}][\text{M}(\text{CO})_5\text{I}]$. Oxidation of $[\text{M}(\text{CO})_5\text{I}]^-$ with elemental iodine liberates carbon monoxide in a vigorous reaction, forming the $\text{M}(\text{II})$ and $\text{W}(\text{II})$ complexes $[\text{R}_4\text{N}][\text{M}(\text{CO})_4\text{I}_3]$. Anion metathesis of the tetracarbonyl triiodide complexes with 2 equiv of sodium dialkyldithiocarbamate produces $\text{Mo}(\text{CO})_2(\text{S}_2\text{CNR}_2)_2^{16}$ and $\text{W}(\text{CO})_3(\text{S}_2\text{CNR}_2)_2$. Advantages of this route over the preparation reported by Colton³ and by Templeton⁴ are as follows:

- (1) Substitution of $\text{M}(\text{CO})_6$ by I^- as a first step allows use of the milder oxidant, iodine, affording a cleaner oxidation of $\text{M}(0)$ to $\text{M}(\text{II})$ as compared with Cl_2 or Br_2 oxidations of $\text{M}(\text{CO})_6$.
- (2) Iodine, a crystalline solid, is more easily used than chlorine gas or liquid bromine.
- (3) Both metal carbonyls, $[\text{R}_4\text{N}][\text{M}(\text{CO})_5\text{I}]$ and $[\text{R}_4\text{N}][\text{M}(\text{CO})_4\text{I}_3]$, are stable salts that are easily isolated and conveniently stored. In contrast, $[\text{M}(\text{CO})_4\text{X}_2]$ ($\text{X} = \text{Cl}, \text{Br}$) starting materials used in earlier preparations must be consumed immediately after generation.¹⁷

Scheme I



The utility of this preparation extends to substituted derivatives of $\text{Mo}(\text{CO})_2(\text{S}_2\text{CNR}_2)_2$ and $\text{W}(\text{CO})_3(\text{S}_2\text{CNR}_2)_2$ such as $\text{M}(\text{CO})(\text{alkyne})(\text{S}_2\text{CNR}_2)_2$, $\text{M}(\text{CO})_2(\text{S}_2\text{CNR}_2)_2\text{L}$, and $\text{M}(\text{alkyne})_2(\text{S}_2\text{CNR}_2)_2$. A disadvantage of this route exists when the electronic character of the dithiocarbamate significantly increases the electrophilicity of $\text{Mo}(\text{CO})_2(\text{S}_2\text{CNR}_2)_2$ since the complex then adds the free iodide liberated in the S_2CNR_2 substitution.

Addition of $[\text{Et}_4\text{N}][\text{F}]$ or $[\text{PPN}][\text{N}_3]$ ($\text{PPN} = \text{bis}(\text{triphenylphosphine})\text{nitrogen}(1+)$) to $\text{M}(\text{CO})_2(\text{S}_2\text{CNR}_2)_2$ ($\text{M} = \text{Mo}, \text{W}$) readily forms $[\text{M}(\text{CO})_2(\text{S}_2\text{CNR}_2)_2\text{F}]^-$ or $[\text{M}(\text{CO})_2(\text{S}_2\text{CNEt}_2)_2\text{N}_3]^-$, respectively. This behavior contrasts with that of remaining members of the halide group. We have reported the nominal propensity of the electron-deficient $\text{Mo}(\text{CO})_2(\text{S}_2\text{CNR}_2)_2$ reagents to add Cl^- and Br^- and the lack of any observable adduct formation with I^- .⁵ Indeed, F^- is the only halide

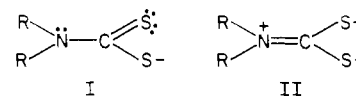
Table III. Infrared Data for $\text{Mo}(\text{CO})_2(\text{S}_2\text{CNR}_2)_2\text{L}$ Complexes

complex	$\nu_{\text{CO}},^a \text{ cm}^{-1}$	$\nu_{\text{CN}},^b \text{ cm}^{-1}$
$\text{Mo}(\text{CO})_2(\text{S}_2\text{CNR}_2)_2$	1933, 1850	1502
$[\text{Et}_4\text{N}][\text{Mo}(\text{CO})_2(\text{S}_2\text{CNR}_2)_2\text{F}]$	1893, 1806	1487
$[\text{PPN}][\text{Mo}(\text{CO})_2(\text{S}_2\text{CNR}_2)_2\text{N}_3]$	1908, 1818	1485
$[\text{Et}_4\text{N}][\text{Mo}(\text{CO})_2(\text{S}_2\text{CNR}_2)_2\text{Cl}]$	1908, 1813	
$[\text{Et}_4\text{N}][\text{Mo}(\text{CO})_2(\text{S}_2\text{CNR}_2)_2\text{Br}]$	1908, 1810	
$\text{Mo}(\text{CO})_2(\text{S}_2\text{CNR}_2)_2\text{PPh}_3$	1935, 1847	1492
$\text{Mo}(\text{CO})_2(\text{S}_2\text{CNR}_2)_2\text{py}$	1920, 1835	

^a In CH_2Cl_2 solution. ^b Solid state in KBr.

to permit isolation of a seven-coordinate complex anion. $[\text{Et}_4\text{N}][\text{M}(\text{CO})_2(\text{S}_2\text{CNEt}_2)_2\text{F}]$ ($\text{M} = \text{Mo}$ (**1**); $\text{M} = \text{W}$ (**2**)) is an orange solid, highly reactive with oxygen and moisture. Whereas an excess of $[\text{Et}_4\text{N}][\text{F}]$ is required to completely generate fluorides **1** and **2**, 1 equiv of $[\text{PPN}][\text{N}_3]$ in an analogous addition reaction instantaneously yields $[\text{PPN}][\text{M}(\text{CO})_2(\text{S}_2\text{CNEt}_2)_2\text{N}_3]$ ($\text{M} = \text{Mo}$ (**3**); $\text{M} = \text{W}$ (**4**)), illustrating the greater metal affinity of the pseudohalide azide ion. Though azide is commonly observed as a bridging ligand, it prefers a terminal ligating role in these systems. Addition of $1/2$ equiv of $[\text{PPN}][\text{N}_3]$ shows only a 50% conversion to product as monitored by observation of ν_{CO} in the infrared spectrum. This experimental result discounts the possibility that the isolated species is an azide-bridged dimer, $[\text{PPN}][(\text{S}_2\text{CNR}_2)_2(\text{CO})_2\text{M}-\text{N}_3-\text{M}(\text{CO})_2(\text{S}_2\text{CNR}_2)_2]$. Ligand-bridged dimers of $\text{M}(\text{II})$ dithiocarbamates exist as exemplified by $(\text{S}_2\text{CNR}_2)_2(\text{CO})_2\text{Mo}-\text{NH}_2\text{NH}_2-\text{Mo}(\text{CO})_2(\text{S}_2\text{CNR}_2)_2$, reported by Broomhead and co-workers.¹⁸ Both fluoride and azide in complexes **1-4** are labile to ligand substitution by phosphines and carbon monoxide to generate neutral $\text{M}(\text{CO})_2(\text{S}_2\text{CNR}_2)_2$ (PR_3) and $\text{M}(\text{CO})_3(\text{S}_2\text{CNR}_2)_2$.

Infrared Data. Formation of $[\text{M}(\text{CO})_2(\text{S}_2\text{CNR}_2)_2\text{X}]^-$ ($\text{X} = \text{F}, \text{N}_3$) can easily be followed spectroscopically due to the 50-cm^{-1} shift in frequency of the two ν_{CO} bands (see Table III). This considerable shift to lower energy seems to result from a net increase in negative charge on the complex rather than increased electron density obtained through coordination of a seventh ligand. For example, $\text{Mo}(\text{CO})_2(\text{S}_2\text{CNR}_2)_2(\text{py})$ has carbonyl stretches only 15 cm^{-1} lower than the dicarbonyl dithiocarbamate complex while $[\text{Mo}(\text{CO})_2(\text{S}_2\text{CNR}_2)_2\text{Br}]^-$ displays a marked decrease in ν_{CO} . The dithiocarbamate ν_{CN} in the 1500-cm^{-1} region is diagnostic for the relative contributions of resonance forms I and II.



The 10-cm^{-1} decrease in ν_{CN} observed in solid-state spectra of **1-4** is consistent with a decreasing contribution from resonance form II due to saturation of the metal by coordination of a seventh ligand. In **1** and **2** the $\text{M}-\text{F}$ vibration appears at 413 cm^{-1} ($\text{M} = \text{Mo}$) and 420 cm^{-1} ($\text{M} = \text{W}$). These low values are in the range normally assigned to bridging fluoride interactions in binary carbonyl fluorides of metals in oxidation state +3 and higher.¹⁹ A paucity of well-characterized low-valent group 6³⁴ fluorides hinders interpretation of our ν_{MF} values. One example of a terminal fluoride bound to a low-valent third-row metal is $\text{Ir}(\text{CO})(\text{PPh}_3)_2\text{F}$, where ν_{MF} is reported at 451 cm^{-1} ,²⁰ a value comparable to those of **1** and **2**.

Description of the Structure of $[\text{Et}_4\text{N}][\text{Mo}(\text{CO})_2(\text{S}_2\text{CNEt}_2)_2\text{F}]$. The molecular symmetry of $[\text{Et}_4\text{N}][\text{Mo}(\text{CO})_2(\text{S}_2\text{CNEt}_2)_2\text{F}]$ approximates C_{2v} , with the C_2 axis along the $\text{Mo}-\text{F}$ bond and bisecting the angle between carbonyl ligands. **1** crystallizes in a monoclinic lattice of $P2_1/n$ symmetry and occupies the four general positions in the cell. Atomic positional parameters are listed in Table IV, and intramolecular bond distances and angles are reported in Tables V and VI, respectively. An ORTEP drawing of the salt is

- (15) (a) Hoffmann, R. *J. Chem. Phys.* **1963**, *39*, 1397. (b) Burdett, J. K. "Molecular Shapes"; Wiley-Interscience: New York, 1980; p 28. (c) Hoffmann, R.; Kubacek, P. *J. Am. Chem. Soc.* **1981**, *103*, 4320.
- (16) $\text{Mo}(\text{CO})_3(\text{S}_2\text{CNR}_2)_2$ is first generated during the $\text{S}_2\text{CNR}_2/\text{I}$ exchange but spontaneously loses CO to give the unsaturated $\text{Mo}(\text{CO})_2(\text{S}_2\text{CNR}_2)_2$. See ref 3 and 4.
- (17) This route follows $\text{M}(\text{CO})_6 + \text{X}_2 \rightarrow [\text{M}(\text{CO})_4\text{X}_2] \rightarrow \text{M}(\text{CO})_3(\text{S}_2\text{CNR}_2)_2$. (a) Anker, M. W.; Colton, R.; Tomkins, I. B. *Aust. J. Chem.* **1967**, *20*, 9. (b) Broomhead, J. A.; Budge, J.; Grumley, W. *Inorg. Synth.* **1976**, *16*, 235.

- (18) Broomhead, J. A.; Budge, J.; Enemark, J. H.; Feltham, R. D.; Gelder, J. I.; Johnson, P. L. *Adv. Chem. Ser.* **1977**, *162*, 421.
- (19) (a) Misra, S. *J. Sci. Ind. Res.* **1981**, *40*, 709. (b) O'Donnell, T. A.; Phillips, K. A. *Inorg. Chem.* **1970**, *9*, 2611.
- (20) Vaska, L.; Peone, J. *Inorg. Synth.* **1975**, *15*, 64.

Table IV. Final Atomic Positional Parameters for [Et₄N][Mo(CO)₂(S₂CNEt₂)₂F]

atom	x	y	z
Mo	-0.01744 (5) ^a	0.16067 (4)	0.24134 (3)
S1	-0.2366 (2)	0.1520 (1)	0.1936 (1)
S2	-0.0779 (2)	0.2780 (1)	0.1404 (1)
S3	0.0593 (2)	0.0250 (1)	0.3043 (1)
S4	0.2102 (2)	0.1547 (1)	0.2472 (1)
F	0.0031 (3)	0.0954 (2)	0.1312 (2)
O1	-0.1388 (4)	0.1540 (3)	0.4138 (3)
O2	0.0376 (5)	0.3147 (3)	0.3533 (3)
N1	-0.3019 (5)	0.2607 (4)	0.0733 (3)
N2	0.2900 (5)	-0.0004 (4)	0.2815 (4)
N3	0.6217 (5)	0.3585 (3)	0.4089 (3)
C1	-0.0938 (5)	0.1564 (4)	0.3497 (4)
C2	0.0182 (6)	0.2569 (4)	0.3103 (4)
C3	-0.2164 (6)	0.2344 (4)	0.1281 (3)
C4	-0.4211 (6)	0.2213 (5)	0.0677 (4)
C5	-0.5049 (7)	0.2553 (6)	0.1316 (6)
C6	-0.2778 (7)	0.3301 (5)	0.0139 (4)
C7	-0.3303 (9)	0.4110 (6)	0.0390 (5)
C8	0.1981 (6)	0.0541 (4)	0.2781 (4)
C9	0.2756 (7)	-0.0942 (6)	0.3002 (5)
C10	0.2872 (8)	-0.1051 (6)	0.3890 (6)
C11	0.4211 (9)	0.0323 (7)	0.2730 (8)
C12A	0.494 (2)	0.021 (1)	0.314 (1)
C12B	0.433 (2)	0.026 (1)	0.206 (2)
C13	0.6202 (2)	0.2815 (5)	0.4632 (4)
C14	0.5725 (8)	0.2051 (5)	0.4171 (5)
C15	0.4999 (7)	0.3750 (5)	0.3692 (4)
C16	0.3955 (7)	0.3725 (5)	0.4281 (5)
C17	0.6576 (7)	0.4326 (5)	0.4660 (4)
C18	0.7835 (8)	0.4276 (6)	0.5027 (6)
C19	0.7109 (6)	0.3453 (5)	0.3396 (4)
C20	0.7302 (7)	0.4206 (5)	0.2854 (4)

^aNumbers in parentheses are the estimated standard deviations of the coordinates and refer to the last significant digit of the preceding number.

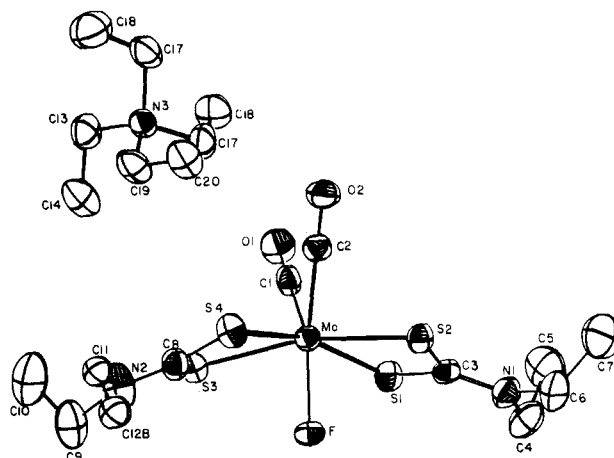
Table V. Intramolecular Bond Distances (Å) for [Et₄N][Mo(CO)₂(S₂CNEt₂)₂F]

Mo-S1	2.538 (2)	Mo-C1	1.942 (6)
Mo-S2	2.545 (2)	Mo-C2	1.925 (6)
Mo-S3	2.530 (2)	C1-O1	1.149 (5)
Mo-S4	2.539 (2)	C2-O2	1.166 (6)
Mo-F	2.055 (3)	C1...C2	2.145 (9)
N3-C13	1.506 (7)	C13-C14	1.515 (9)
N3-C15	1.500 (7)	C15-C16	1.516 (8)
N3-C17	1.537 (8)	C17-C18	1.504 (9)
N3-C19	1.521 (7)	C19-C20	1.501 (8)
S1-C3	1.699 (6)	N2-C9	1.544 (10)
S2-C3	1.701 (6)	N2-C11	1.564 (8)
S3-C8	1.681 (7)	C4-C5	1.503 (9)
S4-C8	1.692 (7)	C6-C7	1.484 (10)
N1-C3	1.337 (6)	C9-C10	1.419 (9)
N1-C4	1.472 (7)	C11-C12A	1.03 (3)
N1-C6	1.487 (8)	C11-C12A	1.08 (5)
N2-C8	1.347 (7)		

provided in Figure 1. The successful structural determination of **1** places it in an elite class of structurally characterized transition-metal carbonyl fluorides; related examples are [Re(CO)(NO)FL₃]⁺,²¹ Re(CO)₅(μ-F)Re(F)₅,²² and [Ru(CO)₃F₂]₄.²³ We are aware of only one other carbonyl fluoride of a group 6 metal that has been structurally characterized, [Mo(CO)₂(dppe)₂F][PF₆]**(5)**.²⁴ The geometries exhibited by **1** and **5** are

Table VI. Selected Bond Angles (deg) in [Et₄N][Mo(CO)₂(S₂CNEt₂)₂F]

Bond Angles for the Anion			
S1-Mo-S2	67.74 (5)	S1-Mo-S4	163.85 (5)
S3-Mo-S4	68.20 (6)	S2-Mo-S4	164.13 (5)
S1-Mo-S3	112.33 (6)	S2-Mo-S3	107.10 (6)
S1-Mo-F	81.50 (9)	S3-Mo-C1	79.93 (19)
S2-Mo-F	82.93 (9)	S4-Mo-C1	115.68 (16)
S3-Mo-F	81.43 (9)	S1-Mo-C2	113.07 (19)
S4-Mo-F	82.67 (10)	S-Mo-C2	79.02 (18)
S1-Mo-C1	79.37 (16)	S3-Mo-C2	113.90 (18)
S2-Mo-C1	117.84 (18)	S4-Mo-C2	79.75 (19)
C1-Mo-C2	67.4 (3)	C2-Mo-F	149.7 (2)
C2-Mo-F	142.9 (2)		
Mo-S1C3	89.6 (2)	Mo-S3-C8	88.0 (2)
Mo-S2-C3	89.3 (2)	Mo-S4-C8	87.5 (2)
C3-N1-C4	121.7 (6)	C8-N2-C9	123.8 (6)
C3-N1-C6	120.5 (6)	C8-N2-C11	119.4 (9)
C4-N1-C6	117.7 (5)	C9-N2-C11	116.6 (8)
S1-C3-S2	112.8 (3)	N1-C4-C5	112.6 (6)
S1-C3-N1	122.4 (5)	N1-C6-C7	113.8 (6)
S2-C3-N1	124.7 (5)		
S3-C8S4	114.8 (4)	N2-C9-C10	107.6 (8)
S3-C8-N2	121.0 (6)	N2-C11-C12A	127 (2)
S4-C8-N2	124.2 (6)	N2-C11-C12B	101 (3)
Bond Angles for the Cation			
C13-N3-C15	110.8 (5)	C13-N3-C19	108.5 (5)
C15-N3-C17	109.0 (5)	N2-C13-C14	113.5 (5)
C17-N3-C19	111.6 (5)	N3-C15-C16	116.3 (5)
C13-N3-C17	107.8 (5)	N3-C17-C18	114.1 (6)
C15-N3-C19	109.1 (5)	N3-C19-C20	114.2 (5)

**Figure 1.** Molecular structure of [Et₄N][Mo(CO)₂(S₂CNEt₂)₂F].

nearly identical and approximate a capped trigonal prism. Fluoride is the capping ligand in both complexes, lying over the face formed by the four dithiocarbamate sulfurs in **1** and by the four dppe phosphorus nuclei in **5**. The four sulfur atoms of **1** are coplanar (± 0.002 Å) and have nearly equivalent Mo-S distances and chelate bite angles; the Mo atom sits 0.35 Å above this plane. The dihedral angle between dithiocarbamate planes is 161°, slightly larger than the corresponding dppe dihedral of 158° in **5**. Note that the Mo-S distances average 2.529 Å, 0.08 Å longer than the average in Mo(CO)₂(S₂CNR₂)₂, in accord with the reduced importance of dithiocarbamate π donation in **1**. A surprising feature of both **1** and **5** is the unusually small angle between carbonyl ligands, 68.2 and 67.4°, respectively. We attribute this acute angle in **1** to the symmetrical trans coordination of fluoride (see Discussion). Both Mo-C and C-O distances are normal, and the Mo-C-O unit is linear. The Mo-F distances in **1** and **5** are similar, 2.055 (3) and 2.035 (6) Å. The nominally shorter distance

(21) Cameron, T. S.; Grundy, K. R.; Robertson, K. N. *Inorg. Chem.* **1982**, *21*, 4149.

(22) Bruce, D. M.; Holloway, J. H.; Russell, D. R. *J. Chem. Soc., Chem. Commun.* **1973**, 321.

(23) Marshall, C. J.; Peacock, R. P.; Russell, D. R.; Wilson, I. L. *J. Chem. Soc., Chem. Commun.* **1980**, 557.

(24) Enemark, J. H.; Chandler, T.; Kriek, G. R. *Cryst. Struct. Commun.* **1980**, 557.

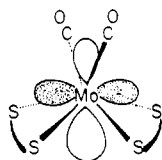


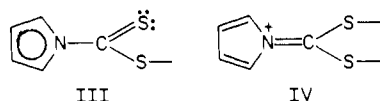
Figure 2. Schematic representation of the $d\pi$ LUMO in $\text{Mo}(\text{CO})_2(\text{S}_2\text{CNR}_2)_2$.

in **5** may be a reflection of the dpp π -acid character and the cationic charge on the complex. The bond distances and angles of both dialkyldithiocarbamate chelates are normal for coordination to $\text{Mo}(\text{II})$. One ethyl group is rotationally disordered (C11, C12A and C12B) and shows suspiciously short C–C bonds and acute angles for sp^3 -hybridized methylene carbon. The tetraethylammonium cation is unremarkable and sits at a noninteracting distance of 3.5 Å from the complex.

Discussion

$\text{Mo}(\text{CO})_2(\text{S}_2\text{CNR}_2)_2$ adopts a trigonal-prismatic geometry to maximize π donation from the π system of the dithiocarbamate chelates as shown in Figure 2. The resulting destabilization of the unfilled and otherwise nonbinding $d_{x^2-y^2}$ orbital accounts for the reluctance of this 16-electron complex to acquire a closed-shell 18-electron configuration.⁴ The modest electrophilicity of $\text{Mo}(\text{CO})_2(\text{S}_2\text{CNR}_2)_2$ permitted us to quantify its affinity for a series of ligands (I^- , Br^- , NCCH_3 , SC_4H_8 , NC_5H_5 , $\text{P}(\text{OR})_3$, PR_3). Equilibrium constant measurements for ligand addition reactions gave large values for phosphine and phosphite ($50\,000\ \text{M}^{-1}$), intermediate values for coordination of heterocycles such as pyridine and tetrahydrothiophene (440, 45 M^{-1}), and near unity for chloride and acetonitrile.⁵ No formation of $[\text{Mo}(\text{CO})_2(\text{S}_2\text{CNR}_2)_2\text{I}]^-$ was observed under excess ligand conditions.

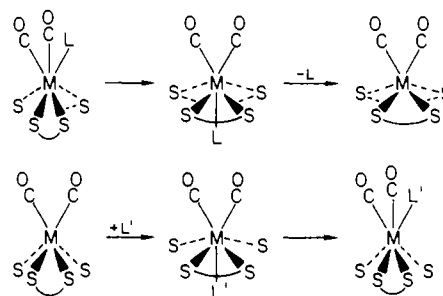
The importance of π donation in increasing the energy of the low-lying LUMO in 16-electron complexes is compatible with the following observations. Replacing the dithiocarbamate alkyl substituents with a pyrrole ring eliminates most of the contribution of resonance structure IV, which is unfavored due to loss of



aromaticity.²⁵ Resonance form III has less π -base character and is not effective in raising the energy of the LUMO in $\text{Mo}(\text{CO})_2(\text{S}_2\text{CNC}_4\text{H}_4)_2$. We observe experimentally that $\text{Mo}(\text{CO})_2(\text{S}_2\text{CNC}_4\text{H}_4)_2$ is a highly electrophilic complex that readily adds iodide or THF.²⁶ Inspection of other 16-electron six-coordinate $\text{Mo}(\text{II})$ complexes such as $[\text{CpMo}(\text{CO})_3]^+$ ²⁷ and $\text{CpW}(\text{CO})_2\text{H}^{28}$ suggests that their extreme reactivity correlates with an absence of π -base ligands.

We have employed frontier orbital theory to predict the site of nucleophilic attack on $\text{Mo}(\text{CO})_2(\text{S}_2\text{CNR}_2)_2$. The most favorable site for attack on the $d_{x^2-y^2}$ -based LUMO appears to be trans to the two carbonyl ligands between the dithiocarbamate planes. EHMO calculations reveal that the LUMO (Figure 2) has a disproportionately large lobe extending in the $+x$ direction due to some $\text{Mo } p_x$ -orbital mixing. This swollen but vacant lobe lies between the wings defined by the dihedral angle of 135° between the dithiocarbamate planes. Indeed, a trans location of a seventh ligand was observed in the single-crystal X-ray study of $\text{Mo}(\text{CO})_2(\text{S}_2\text{CNR}_2)_2(\text{tht})$ (tht = tetrahydrothiophene) (**6**).⁵ The tht adduct was selected for study with the hope that its weak interaction with molybdenum, as manifested by dissociation in the absence of tht vapor, might reflect the site of attack. The Mo – S bond length of 2.70 Å in **6** verifies a weak interaction, with

Scheme II



the thioether located in an unsymmetrical trans position relative to the carbonyl ligands ($\text{OC-Mo-S} = 178, 113^\circ$).

The trend in equilibrium data for halides ($\text{I}^- < \text{Br}^- < \text{Cl}^-$) suggested that fluoride might have the highest stability constant for coordination to $\text{Mo}(\text{CO})_2(\text{S}_2\text{CNR}_2)_2$. Although a K_{eq} value could not be obtained due to solubility complications, qualitatively fluoride binds more tightly than pyridine. The choice of fluoride as seventh ligand in a structural comparison with carbon monoxide and phosphine analogues provided an opportunity to delineate the importance of π effects for geometric preferences.

Figure 1 illustrates the capped-trigonal-prismatic geometry adopted by **1**. The Mo-F bond does not produce a mutually *cis*- $\text{M}(\text{CO})_2\text{L}$ unit. The π -acid character of CO and PPh_3 may well be the dominant factor favoring a *cis*- $\text{M}(\text{CO})_2\text{L}$ unit in $\text{M}(\text{CO})_2\text{L}(\text{S}_2\text{CNR}_2)_2$ complexes with $\text{L} = \text{CO}, \text{PPh}_3$.

The structure of **1** reflects fluoride addition to the $d_{x^2-y^2}$ -dominated LUMO of $\text{Mo}(\text{CO})_2(\text{S}_2\text{CNR}_2)_2$. Various mechanistic proposals are compatible with the data available for formation of $\text{ML}(\text{CO})_2(\text{S}_2\text{CNR}_2)_2$ compounds. We suggest a mechanistic model based on three assumptions that are intuitively attractive though unproven: (i) $\text{Mo}(\text{CO})_2(\text{S}_2\text{CNR}_2)_2$ will react as an electrophile toward potential ligands including F^- , CO , PPh_3 , etc. (ii) Even for π -acid ligands such as CO and PPh_3 , the initial interaction of free L with $\text{Mo}(\text{CO})_2(\text{S}_2\text{CNR}_2)_2$ will be with L acting as an electron-pair donor with π bonding playing a secondary role of growing importance as the adduct forms and adopts its ground-state geometry. (iii) Seven-coordinate species are more likely to undergo facile rearrangement than are six-coordinate species.

These premises lead us to suggest that incoming ligands initially add to $\text{Mo}(\text{CO})_2(\text{S}_2\text{CNR}_2)_2$ in the cleft between the chelating ligands trans to the carbonyls. Nuclear motion along the soft energy surface of $\text{M}(\text{CO})_2\text{L}(\text{S}_2\text{CNR}_2)_2$ then leads to one of the three basic ground-state structures: *cis*- $\text{M}(\text{CO})_2\text{L}$; L symmetrically opposite both CO 's; L asymmetrically opposite both CO 's and roughly trans to one CO . Application of the principle of microscopic reversibility to dissociative-substitution reactions of *cis*- $\text{M}(\text{CO})_2\text{L}(\text{S}_2\text{CNR}_2)_2$ compounds in this framework requires rearrangement to a *trans*- $\text{M}(\text{CO})_2\text{L}$ geometry prior to loss of L to form $\text{Mo}(\text{CO})_2(\text{S}_2\text{CNR}_2)_2$. Scheme II diagrams such a reaction mechanism.

General features may be extracted from Scheme II that are germane to substitution mechanisms in other saturated organometallic systems. Even when the geometries of the reagent and product are nearly identical (as in the formation of $\text{W}(\text{CO})_2(\text{PPh}_3)(\text{S}_2\text{CNR}_2)_2$ from the $\text{W}(\text{CO})_3(\text{S}_2\text{CNR}_2)_2$ reagent), a reaction path of least motion need not apply. The actual mechanism may involve intermediates or transition states whose geometries bear no similarity to reagent or product. For example, in Scheme II the initial step transforms the reagent to the *trans*- $\text{M}(\text{CO})_2\text{L}$ arrangement, which can produce the known $\text{M}(\text{CO})_2(\text{S}_2\text{CNR}_2)_2$ geometry directly upon loss of L in accord with Hammond's postulate.²⁹

One alternative scheme can be based on facile isomerization of the six-coordinate $\text{Mo}(\text{CO})_2(\text{S}_2\text{CNR}_2)_2$ electrophile to present various geometries and acceptor orbitals to the incoming ligand. Another addition route for CO and PPh_3 would be to have them

(25) Bereman, R. D.; Nalewajek, D. *Inorg. Chem.* **1977**, *16*, 2687.

(26) (a) Herrick, R. S.; Templeton, J. L., manuscript in preparation. (b) Herrick, R. S.; Burgmayer, S. J. N.; Templeton, J. L. *Inorg. Chem.* **1983**, *22*, 3275.

(27) Beck, W.; Schloter, K. Z. *Naturforsch., B: Anorg. Chem., Org. Chem.* **1978**, *33B*, 1214.

(28) Kazlauskas, R. J.; Wrighton, M. S. *J. Am. Chem. Soc.* **1980**, *102*, 1727.

(29) Hammond, G. S. *J. Am. Chem. Soc.* **1955**, *77*, 334.

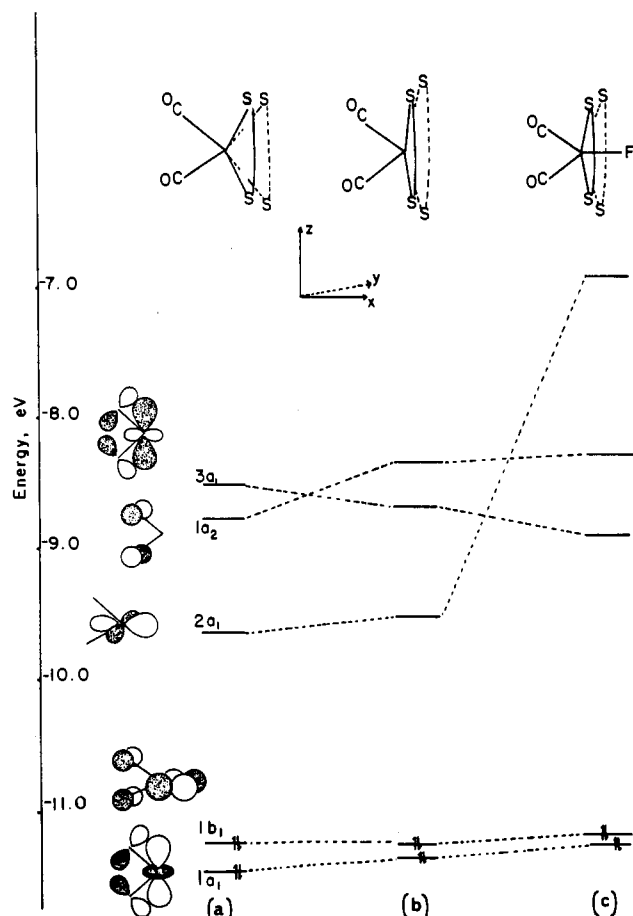


Figure 3. Correlation diagram for the conversion of $\text{Mo}(\text{CO})_2(\text{S}_2\text{CNR}_2)_2$ to $[\text{Mo}(\text{CO})_2(\text{S}_2\text{CNR}_2)_2\text{F}]^-$ with geometries a, b, and c as defined in the Discussion. Note that the symmetry labels are those of the C_{2v} point group with x as the axis of quantization as defined in the coordinate system shown.

approach in a manner that would optimize donation of metal $d\pi$ electron density into an empty π orbital of the attacking ligand. We feel these proposals are less likely than Scheme II, but they are nonetheless viable alternatives.

A structural feature common to seven-coordinate Mo(II) and W(II) complexes is an angle near 70° between carbonyl ligands. The 26 acute OC-M-CO angles listed by Day, Batschelet, and Archer for seven-coordinate carbonyl compounds average $73 \pm 2^\circ$ with 19 falling in the $71\text{--}75^\circ$ range.³⁰ The occurrence of these angles might be naively rationalized in terms of increased congestion accompanying high coordination numbers. Note, however, that eight-coordinate Mo(IV) and W(IV) dicarbonyls exhibit OC-M-CO angles near 90° as a consequence of maximizing metal $d\pi$ delocalization into CO π^* orbitals.³¹ Accordingly, $\text{Mo}(\text{CO})_2(\text{S}_2\text{CNR}_2)_2$ ⁴ and adducts with tht ,⁵ CO ,⁸ and PPh_3 ⁹ have dicarbonyl angles of 74.3 , 73.5 , 71.7 , and 71.6° , respectively. Anticipating a similar value for the OC-Mo-CO angle in **1**, we were surprised to find a value of 67.4° and a carbon-carbon separation of only 2.14 \AA between the carbonyl ligands. The relevance of acute angles to carbon-carbon bond formation via reductive carbonyl coupling has been treated theoretically.¹⁰ **1** presented an opportunity to try to identify some of the factors favoring decreased OC-M-CO angles in seven-coordinate bis(dithiocarbamate) complexes.

Extended Hückel calculations were performed on three model complexes: (a) $\text{Mo}(\text{CO})_2(\text{S}_2\text{CNH}_2)_2$, (b) $\text{Mo}(\text{CO})_2(\text{S}_2\text{CNH}_2)_2$ with the geometry of a compressed trigonal prism derived by removal of F^- from model c, and (c) $[\text{Mo}(\text{CO})_2(\text{S}_2\text{CNH}_2)_2\text{F}]^-$.

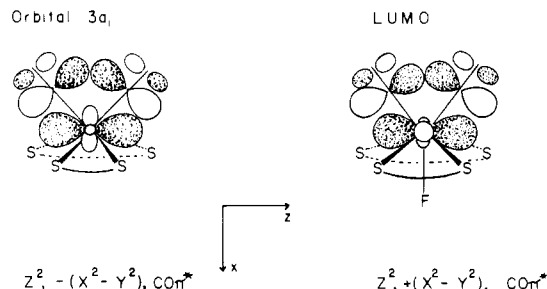
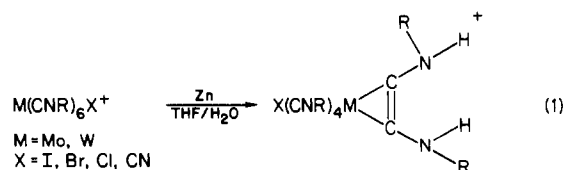


Figure 4. Schematic representation of the transformation of $3a_1$ in $\text{Mo}(\text{CO})_2(\text{S}_2\text{CNR}_2)_2$ into the LUMO of $[\text{Mo}(\text{CO})_2(\text{S}_2\text{CNR}_2)_2\text{F}]^-$.

Calculations on models a and c employed available crystallographic positions. The abbreviated correlation diagram in Figure 3 summarizes the pertinent results. The two filled orbitals $1a_1$ and $1b_1$ have predominately M-CO π^* character due to the symmetry match of $d_{xy}(b_1)$ and $d_{z^2}(a_1)$ with CO π^* orbitals parallel to the xy and xz planes, respectively. No significant energy changes occur along the reaction path for these two when the dithiocarbamate ligands are flexed to 161° preceding fluoride coordination. An important consequence of F^- interacting with $d_{x^2-y^2}$ is a different mixing of d_{z^2} and $d_{x^2-y^2}$ in filled orbitals; the effect of this compositional change is more clearly reflected in the antisymmetric counterparts of these orbitals (vide infra). Orbital $2a_1$, the LUMO for both unsaturated structures, is primarily $d_{x^2-y^2}$. The dithiocarbamate π donation in $2a_1$ (not included in the diagram for clarity; see Figure 2) is enhanced in intermediate structure b, and $2a_1$ rises slightly in energy. Upon coordination of fluoride, this orbital predictably zooms to higher energies, consistent with acquisition of Mo-F σ^* character. Antisymmetric carbonyl π^* combinations parallel to the xy plane are the sole component of orbital $1a_2$, which increases in energy as the angle between dithiocarbamate ligands opens, but it is almost unaffected by fluoride addition. The other empty orbital shown, $3a_1$, possesses primarily M-CO π^* character and is the antibonding partner to $1a_1$. Originating as a composite of d_{z^2} and CO π^* in the xz plane with some $d_{x^2-y^2}$, it responds to flexing of the chelate ligands by descending in energy and terminates as the LUMO for saturated **1**. $3a_1$ mirrors the aforementioned orbital redistribution occurring within $1a_1$. Comparative diagrams of $3a_1$ before and after reaction are shown in Figure 4. The critical yet subtle transformation of $3a_1$ is due to a sign reversal for the $d_{x^2-y^2}$ component of the wave function. Mixing a small amount of $d_{x^2-y^2}$ into d_{z^2} deforms the nodal cone of d_{z^2} , schematically exaggerated in Figure 4. We believe that this phase change is responsible for the acute angle of **1**; the OC-Mo-CO angle adjusts to the decreasing d_{z^2} nodal angle to optimize σ bonding into the nodes and π back-bonding from the metal.

Shifting attention to the carbonyl π^* system is $3a_1$, we find a constructive overlap between the cis carbonyl monoxide carbon atoms. Adding an electron pair to the LUMO could conceivably promote C-C bond formation and generate an acetylene diolate ligand. A closely related reductive coupling reaction that occurs in seven-coordinate molybdenum or tungsten isocyanides has been examined by Lippard (eq 1).³² Several parallels exist between



1 and $[\text{M}(\text{CNR})_6\text{I}]^-$ that suggest an analogous reductive carbonyl coupling for **1** may be possible: (a) both structures are seven-coordinate d^4 complexes with a capped-trigonal-prismatic geometry and (b) both systems have a halide ligand trans to the two π acids

(30) Day, R. O.; Batschelet, W. H.; Archer, R. D. *Inorg. Chem.* **1980**, 2127.

(31) Erler, B. S.; Dewan, J. C.; Lippard, S. J.; Tyler, D. R. *Inorg. Chem.* **1981**, 20, 2719.

(32) Giandomenico, C. M.; Lam, C. T.; Lippard, S. J. *J. Am. Chem. Soc.* **1982**, 104, 1263.

forming an acute angle (69° in the isocyanides). Reduction of **1** and **2** with Zn dust in acetonitrile occurs under mild reflux, but the reduction promotes loss of a chelate ligand to ultimately yield $[\text{Mo}(\text{CO})_4(\text{S}_2\text{CNR}_2)]^-$.

The low ν_{MoF} stretching frequency and the Mo-F bond distance suggest a weak M-F interaction relative to that in higher oxidation state metal fluoride complexes where fluoride π donation to the metal can strengthen the Mo-F bond. Verification of no significant F $p\pi$ -Mo $d\pi$ interaction was gleaned from inspection of proper orbitals in the EHMO calculation. An absence of π donation in 18-electron fluoride complexes has been observed by Crabtree.³³

In summary, this work exploits the structure of a seven-coordinate dicarbonyl fluoride of Mo(II) to suggest a frontier-con-

trolled ligand substitution mechanism in saturated Mo(II) and W(II) systems and to decipher ligand properties responsible for determining the final geometry. We have also probed factors promoting acute angles in bis chelate dicarbonyl halides with capped-trigonal-prismatic geometries through a theoretical (EHMO) study of fluoride complex **1**.

Acknowledgment. This work was supported by NSF Grant CHE8310121. We are grateful to Professor D. J. Hodgson for providing crystallographic expertise and to Professor J. H. Enemark for helpful discussions of alternate reaction pathways.

Registry No. **1**, 96394-35-3; **2a**, 96394-37-5; **2b**, 96427-14-4; **3**, 96394-39-7; **4**, 96394-41-1; $\text{Mo}(\text{CO})_2(\text{S}_2\text{CNMe}_2)_2$, 80664-77-3; $\text{Mo}(\text{CO})_2(\text{S}_2\text{CNET}_2)_2$, 74807-43-5; $[\text{Et}_4\text{N}][\text{Mo}(\text{CO})_5\text{I}]$, 14781-00-1; $\text{Mo}(\text{CO})_6$, 13939-06-5; $[\text{Et}_4\text{N}][\text{W}(\text{CO})_5\text{I}]$, 14781-01-2; $\text{W}(\text{CO})_6$, 14040-11-0; $\text{W}(\text{CO})_3(\text{S}_2\text{CNMe}_2)_2$, 72881-01-7; $\text{W}(\text{CO})_3(\text{S}_2\text{CNET}_2)_2$, 72827-54-4; $\text{W}(\text{CO})_2(\text{S}_2\text{CNMe}_2)_2$, 69916-43-4; $\text{W}(\text{CO})_2(\text{S}_2\text{CNET}_2)_2$, 82284-90-0; $\text{Mo}(\text{CO})_2(\text{S}_2\text{CNH}_2)_2$, 80004-29-1; $[\text{Mo}(\text{CO})_2(\text{S}_2\text{CNH}_2)_2\text{F}]^-$, 96427-15-5.

Supplementary Material Available: Tables of thermal parameters, calculated hydrogen positions, and observed and calculated structure factors (Tables VII, VIII, and IX, respectively) (21 pages). Ordering information is given on any current masthead page.

(33) Crabtree, R. H.; Hlatky, G. G.; Holt, E. M. *J. Am. Chem. Soc.* **1983**, *105*, 7302.

(34) In this paper the periodic group notation is in accord with recent actions by IUPAC and ACS nomenclature committees. A and B notation is eliminated because of wide confusion. Groups IA and IIA become groups 1 and 2. The d-transition elements comprise groups 3 through 12, and the p-block elements comprise groups 13 through 18. (Note that the former Roman designation is preserved in the last digit of the new numbering: e.g., III \rightarrow 3 and 13.)

Contribution from the Dipartimento di Chimica dell'Università, Istituto ISSECC, CNR, 50132 Firenze, Italy

Synthesis and Characterization of Dinuclear Metal Complexes with the P_2S and As_2S Heteroatomic Inorganic Rings as Bridging Units. Crystal and Molecular Structure of $[(\text{triphos})\text{Rh}(\text{As}_2\text{S})\text{Rh}(\text{triphos})](\text{BPh}_4)_2 \cdot 2(\text{CH}_3)_2\text{CO}$ [triphos = 1,1,1-Tris((diphenylphosphino)methyl)ethane]

MASSIMO DI VAIRA, FABRIZIO MANI, SIMONETTA MONETI, MAURIZIO PERUZZINI, LUIGI SACCONI, and PIERO STOPPIONI*

Received August 9, 1984

The cobalt complexes $[(\text{triphos})\text{Co}(\text{E}_2\text{S})]\text{BF}_4$ [triphos = 1,1,1-tris((diphenylphosphino)methyl)ethane; E = As, P], containing the heterocyclic diphosphorus-sulfur and diarsenic-sulfur units η^3 coordinated to the metal atom, react with a rhodium(I) complex or with cobalt(II) tetrafluoroborate in the presence of triphos, yielding compounds with the general formula $[(\text{triphos})\text{M}(\text{E}_2\text{S})\text{M}'(\text{triphos})]\text{Y}_2$ (E = As, P; M = M' = Co or M = Co and M' = Rh, Y = BF_4 ; M = M' = Rh, Y = BPh_4). The crystal structure of $[(\text{triphos})\text{Rh}(\text{As}_2\text{S})\text{Rh}(\text{triphos})](\text{BPh}_4)_2 \cdot 2(\text{CH}_3)_2\text{CO}$ has been elucidated through a complete X-ray analysis: triclinic, $a = 19.344$ (9) Å, $b = 18.887$ (9) Å, $c = 19.581$ (10) Å, $\alpha = 122.93$ (9)°, $\beta = 93.56$ (8)°, $\gamma = 95.09$ (8)°, space group $P\bar{1}$, $Z = 2$, $R = 0.083$, 4727 reflections. The complex has a triple-decker sandwich structure with the As_2S unit bridging the two $\text{Rh}(\text{triphos})$ moieties. Such an internal unit, affected by orientational disorder, has the shape of a triangle with two sides [2.34 (1), 2.52 (1) Å] in the range of normal bond lengths and a very long [3.10 (1) Å] side. The same sort of structure is assigned to all of the complexes on the basis of conductivity, spectrophotometric, and magnetic measurements.

Introduction

The cobalt complexes of formula $[(\text{triphos})\text{Co}(\text{E}_2\text{S})]\text{BF}_4$ [triphos = 1,1,1-tris((diphenylphosphino)methyl)ethane; E = As, P], containing the heterocyclic diphosphorus-sulfur or diarsenic-sulfur units η^3 coordinated to the metal atom, have been synthesized and characterized.^{1,2} These compounds have provided the first examples of inorganic heteroatomic three-membered rings π bonded to a metal atom. Such cationic compounds are iso-electronic with the neutral $[(\text{triphos})\text{M}(\text{P}_3)]$ (M = Co, Rh, Ir) complexes,^{3,4} which contain the homocyclic triphosphorus unit. The latter complexes have been found to be capable of reacting with appropriate metal-ligand moieties, affording homo- and

heterometallic sandwich complexes of formula $[(\text{triphos})\text{M}(\text{P}_3)\text{M}'(\text{triphos})]\text{Y}_2$ (M = Co, Rh; M' = Co, Ni, Rh, Ir, Y = BF_4 , PF_6 , BPh_4),^{5,6} in which the *cyclo*-triphosphorus unit bridges two metal atoms.

With the aim to investigate possible effects on the reactivity of the cationic complexes due to the presence of the heteroatom in the triatomic E_2S ring, the $[(\text{triphos})\text{Co}(\text{E}_2\text{S})]\text{BF}_4$ (E = As, P) compounds have been reacted with $\text{Co}(\text{BF}_4)_2 \cdot 6\text{H}_2\text{O}$ and $[\text{RhCl}(\text{cod})]_2$ (cod = cycloocta-1,5-diene) in the presence of triphos. Dinuclear homo- and heterometallic derivatives of formula $[(\text{triphos})\text{M}(\text{E}_2\text{S})\text{M}'(\text{triphos})]\text{Y}_2$ (E = As, P; M = M' = Co or M = Co and M' = Rh, Y = BF_4 ; M = M' = Rh, Y = BPh_4) have been obtained. These complexes, which crystallize with two molecules of acetone, have been characterized by means of magnetic, spectrophotometric, and conductivity measurements.

(1) Di Vaira, M.; Peruzzini, M.; Stoppioni, P. *J. Chem. Soc., Dalton Trans.* **1984**, 359.

(2) Di Vaira, M.; Innocenti, P.; Moneti, S.; Peruzzini, M.; Stoppioni, P. *Inorg. Chim. Acta* **1984**, *83*, 161.

(3) Ghilardi, C. A.; Midollini, S.; Orlandini, A.; Sacconi, L. *Inorg. Chem.* **1980**, *19*, 301.

(4) Bianchini, C.; Mealli, C.; Meli, A.; Sacconi, L. *Inorg. Chim. Acta* **1979**, *37*, L543.

(5) Di Vaira, M.; Midollini, S.; Sacconi, L. *J. Am. Chem. Soc.* **1979**, *101*, 1757.

(6) Bianchini, C.; Di Vaira, M.; Meli, A.; Sacconi, L. *J. Am. Chem. Soc.* **1981**, *103*, 1448.